ANNALS of the ORADEA UNIVERSITY.
Fascicle of Management and Technological Engineering, Volume XI (XXI), 2012, NR1

THEORETICAL CONSIDERATIONS UPON PLASTIC SHEAR REGIONS IN A LUBRICANT FILM PLACED BETWEEN AN ASPERITY AND A PLANE

Vasilache Fomin Michaela
University of Suceava
fomin_michaela@yahoo.com

Keywords: limiting shear stress, shear strength, roughness, pressure distribution.

Abstract: The effect of plastic shear and that of attaining shear strength within the lubricant film upon the bearing capacity of a coupling was studied extensively in literature, [1 - 6]. The present paper proposes a new approach to this problem, by means of studying the lubricated contact between of single prismatic asperity with flat surface. Numerical results highlight the negative effect of roughness upon film thickness, bearing capacity, and shear stress. Some considerations are made on the subject of seizing.

1. MODELING OF AN ASPERITY AS TWO PLANE PAD BEARINGS LUBRICATED BY VISCOUS NEWTONIAN FLUIDS

The present paper highlights the negative effect generated by asperities of a certain shape and size upon lubricant film thickness, pressure distributions and limiting shear stress in hydrodynamic lubrication. Shear stress generated at the asperity level in a hydrodynamic contact can in certain cases exceed the admissible shear limiting stress, known as shear strength, and initiate “tearing” in the lubricant film, [5], continued by film “thinning” until opposite surface asperities touch, and eventually lead to seizing of the bearing.

1.1 PHYSICAL AND MATHEMATICAL MODELING OF ASPERITIES

For the proposed investigations, the simple case of viscous Newtonian fluids was considered. The physical and mathematical model consists of bi-dimensional asperities, modeled by triangles, in contact with a flat surface. The chosen asperity is fixed, while the flat surface, considered smooth, is set in motion with a speed u=U, along the positive direction of x axis. Between the two surfaces, a viscous Newtonian fluid of constant density and viscosity is interposed.

For simplicity, the geometry considered for the asperity, was that of a triangle assimilated to two symmetrical plane pad bearings, as illustrated in Figure 1.

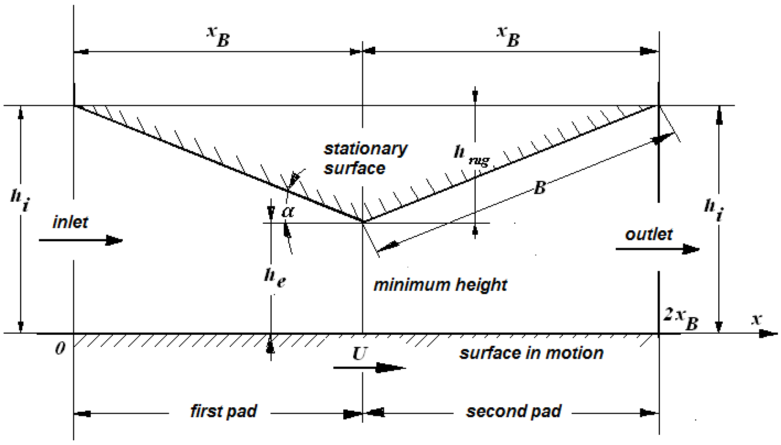

Figure 1. Geometry of a triangular asperity

1.2 ASPERITY GEOMETRY

The geometry of considered asperity is determined by two lines of slopes k_1 and k_2 respectively. Geometrical equations of the two lines, corresponding to the two plane pads, are given by $h_1(x)$, for the inlet pad and $h_2(x)$ for the outlet pad, respectively:

$$h_1(x) = h_i + k_1 x; \tag{0.1}$$

$$h_2(x) = h_e - k_2 x_B + k_2 x. \tag{0.2}$$

By reunion of the two regions delimited by the considered lines, a general equation for the plane pad bearing can be written as:

$$h(x) = \begin{cases} h_1(x), & 0 < x < x_B \\ h_2(x), & x_B < x < 2x_B \end{cases}. \tag{0.3}$$

It can be noticed that:

$$k_1 = -k_2, \tag{0.4}$$

due to plane pad bearing symmetry.

1.3 PRESSURE DISTRIBUTION

The pressure distribution yields from integration of Reynolds one-dimensional equation, specific to hydrodynamic lubrication, given by:

$$\frac{dp(x)}{dx} = \frac{6\eta U(h(x) - h_m)}{h(x)^3}, \tag{0.5}$$

where $h_m = h\left(x_m\right)$, represents the height corresponding to a pressure extreme (a maximum for the first pad and a minimum in the case of the second pad).

Separately, pressure distributions for the two pads have the following expressions:

First pad:

$$p_1(x) = \frac{6\eta U}{k_1}\left(-\frac{1}{h_1(x)} + \frac{h_{m1}}{2h_1(x)^2}\right) + C_1. \tag{0.6}$$

Second pad:

$$p_2(x) = \frac{6\eta U}{k_2}\left(-\frac{1}{h_2(x)} + \frac{h_{m2}}{2h_2(x)^2}\right) + C_2. \tag{0.7}$$

By applying boundary conditions (at the inlet and outlet), it results that:

$$C_1 = \frac{6\eta U}{k_1}\left(\frac{1}{h_i} - \frac{h_{m1}}{2h_i^2}\right), \tag{0.8}$$

for $x = 0,\ h_1(x) = h_i$, where $p_1(x) = 0$,

$$C_2 = \frac{6\eta U}{k_2}\left(\frac{1}{h_i} - \frac{h_{m2}}{2h_i^2}\right), \tag{0.9}$$

for $x = 2x_B$, $h_2(x) = h_i$, where $p_2(x) = 0$.

Flow equations for the two pads can be written as follows:
First pad:

$$Q_1 = -\frac{h_1^3}{12\eta}\frac{dp_1}{dx} + \frac{h_1 U}{2}. \tag{0.10}$$

Second pad:

$$Q_2 = -\frac{h_2^3}{12\eta}\frac{dp_2}{dx} + \frac{h_2 U}{2}. \tag{0.11}$$

The flows are equal at abscises where pressure gradients annul, and it results that:

$$\frac{h_{m1}U}{2} = \frac{h_{m2}U}{2}, \tag{0.12}$$

and consequently

$$h_{m1} = h_{m2} = h_m \tag{0.13}$$

By imposing the second boundary condition, $x = x_B$; $h_1(x) = h_2(x) = h_e$; where $p_1(x_B) = p_2(x_B) = p_e$, it results for the two pads:
First pad:

$$p_e = \frac{6\eta U}{k_1}\left[\frac{1}{h_i} - \frac{1}{h_e} + \frac{h_m}{2}\left(\frac{1}{h_e^2} - \frac{1}{h_i^2}\right)\right] \tag{0.14}$$

Second pad:

$$p_e = \frac{6\eta U}{k_2}\left[\frac{1}{h_i} - \frac{1}{h_e} + \frac{h_m}{2}\left(\frac{1}{h_e^2} - \frac{1}{h_i^2}\right)\right] \tag{0.15}$$

Knowing that $k_1 = -k_2$, and by creating a system with the last two equations (p_e and k_{1m}), it results that:

$$h_m = \frac{2h_i h_e}{h_i + h_e}$$
$$p_e = 0 \tag{0.16}$$

Coefficients, C_1 and C_2, obtained from eq. (1.8) and (1.9), along with height are then introduced in the pressure distribution equations (1.14) and (1.15). Since the heights where pressure gradients annul, are equal, it can be noticed that pressure gradients are also equal in the point that connects the two pads $(h_m = h_{m1} = h_{m2})$. As the tangent to pressure distribution is the same for both pads, it can be concluded that the pressure distribution is continuous in said point. As a result, the pressure distribution along the asperity can be effectively obtained as a reunion of pressure distributions yielded for each pad, according to the following equation:

$$p(x) = \begin{cases} p_1(x) \ , & 0 < x < x_B \\ p_2(x) \ , & x_B < x < 2x_B \end{cases} \tag{0.17}$$

1.4 SPEED DISTRIBUTION

By using the equilibrium equation in the xOz plane for a volume element and the constitutive equation:

$$\frac{dp}{dx} = \frac{\partial \tau}{\partial z}; \qquad \tau = \eta \frac{\partial u}{\partial z} \tag{0.18}$$

and by taking into consideration that viscosity is constant, a differential equation is obtained, that after double integration leads to the following expression:

$$\frac{\partial^2 u}{\partial z^2} = \frac{1}{\eta}\frac{dp}{dx}; \quad u = \frac{1}{2\eta}\frac{dp}{dx} z^2 + C_1 z + C_2 \tag{0.19}$$

where C_1 and C_2 are determined from the boundary conditions:

$$\begin{cases} for \ \ z = 0: \ \ u = U, \ C_2 = U; \\ for \ \ z = h: \ \ u = 0, \ C_2 = -\frac{U}{h} - \frac{1}{\eta}\frac{dp}{dx}\frac{h}{2}; \end{cases} \tag{0.20}$$

By particularization for each pad, the following expressions were determined for speed distributions:

$$u_1 = \frac{1}{2\eta}\frac{dp_1}{dx}(z^2 - zh_1) + U\left(1 - \frac{z}{h_1}\right) \tag{0.21}$$

$$u_2 = \frac{1}{2\eta}\frac{dp_2}{dx}(z^2 - zh_2) + U\left(1 - \frac{z}{h_2}\right) \tag{0.22}$$

Reunion of eqs. (0.21) and (0.22) for the two regions, led to the following speed distribution along the considered asperity:

$$u(x,z) = \begin{cases} u_1(x,z) \ , & 0 < x < x_B \\ u_2(x,z) \ , & x_B < x < 2x_B \end{cases} . \tag{0.23}$$

1.5 FLOW

Volume flow per length unit can be obtained by integration of speed distribution over the lubricant film thickness:

$$Q_v = \int_0^h u(x,z)dz \quad \rightarrow \quad Q_v = -\frac{h_1^3}{12\eta}\frac{dp1}{dx} + \frac{h_1 U}{2} = -\frac{h_2^3}{12\eta}\frac{dp_2}{dx} + \frac{h_2 U}{2} \tag{0.24}$$

Mass flow is then obtained by multiplying the volume flow with density, which was considered constant.

$$Q_m = \rho Q_v \quad \rightarrow \quad Q_m = -\frac{\rho h_1^3}{12\eta}\frac{dp_1}{dx} + \frac{\rho h_1 U}{2} = -\frac{\rho h_2^3}{12\eta}\frac{dp_2}{dx} + \frac{p h_2 U}{2} \tag{0.25}$$

1.6 SHEAR STRESS DISTRIBUTION

Shear stress distribution can be determined by replacing the speed distribution in equation (1.18). Consequently, for the two regions of the asperity, the following relations were obtained:

$$\tau_1 = \frac{dp_1}{dx}\left(z - \frac{h_1}{2}\right) - \frac{\eta U}{h_1} \quad \text{and} \quad \tau_2 = \frac{dp_2}{dx}\left(z - \frac{h_2}{2}\right) - \frac{\eta U}{h_2} \tag{0.26}$$

By combining equation (1.25) for the two regions, the following shear stress distribution was determined along an asperity:

$$\tau(x,z) = \begin{cases} \tau_1(x,z)\ ,\ 0 < x < x_B \\ \tau_2(x,z)\ ,\ x_B < x < 2x_B \end{cases} \tag{0.27}$$

1.7 PARTICULARIZATION

Pressure distributions, pressure gradients, speed and shear stresses were plotted for particular situations. The following variable values were considered as representative:

$U = 10\frac{m}{s}$; $x_B = 0,25 \times 10^{-6} m$, $h_{rug} = 0,5 \times 10^{-6} m$ $h_e = 0,01 \times 10^{-3} m$; $h_i = h_e + h_{rug} = 1,5 \times 10^{-6} m$;

$a = \frac{h_i}{h_e} = 1,5$ $a = \frac{\boldsymbol{h_i}}{\boldsymbol{h_e}} = 1,\mathbf{5}$ (non-dimensional), $k_1 = -k_2$; $\eta = 0,15 Pa \times s$.

A scale representation of an asperity in this particular case is illustrated in Figure 2:

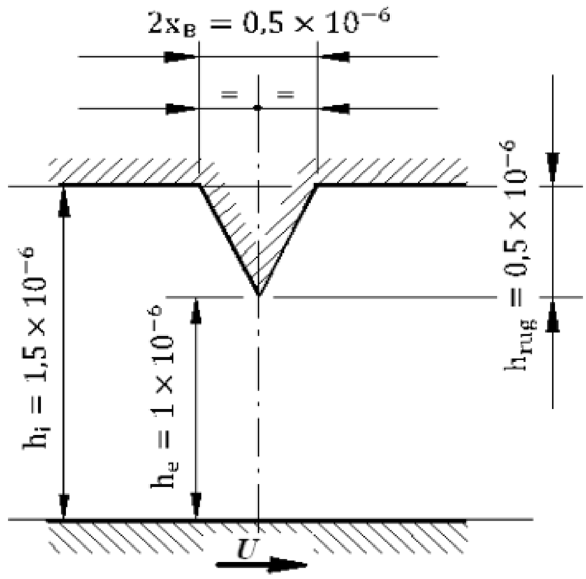

Figure 2. Asperity geometry (scaled representation)

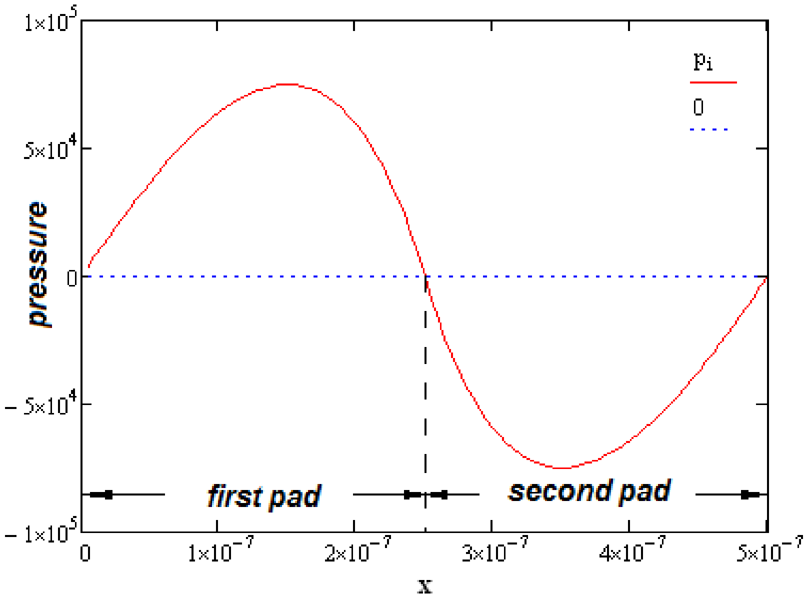

Figure 3. Pressure distribution along the asperity in Figure 2

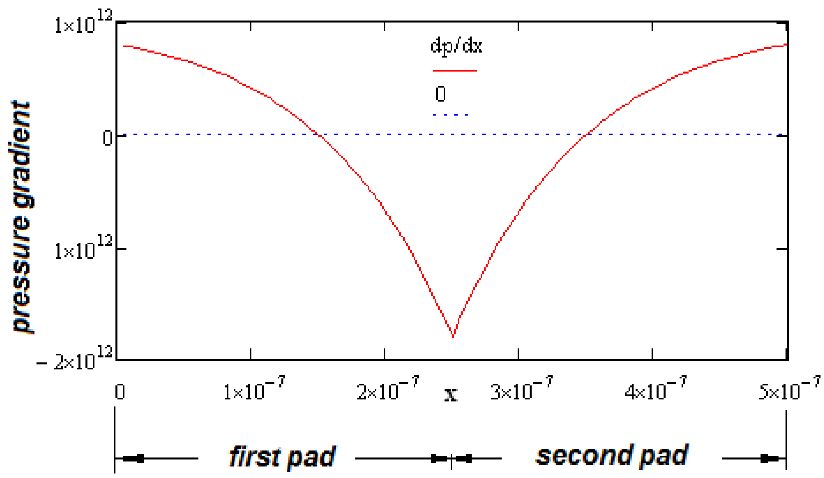

Figure 4. Pressure gradient along the asperity in Figure 2

After an analysis of pressure gradient (Figure 4) and shear stress distributions (Figure 6) at both plane and pad limits, an important discontinuity was found in both plots corresponding to the tip of the asperity. Under real conditions, that would generate turbulent phenomena, but in the case of high viscosity fluids, as is the case with EHL, when lubricant viscosity increases exponentially with pressure according to Barus's law, ($\eta = \eta_0 \exp(\alpha p)$), the fluid has laminar flow. Under these conditions, in order to attenuate the limiting shear stress discontinuities, it is necessary for plastic shear to appear at the tip of the asperity.

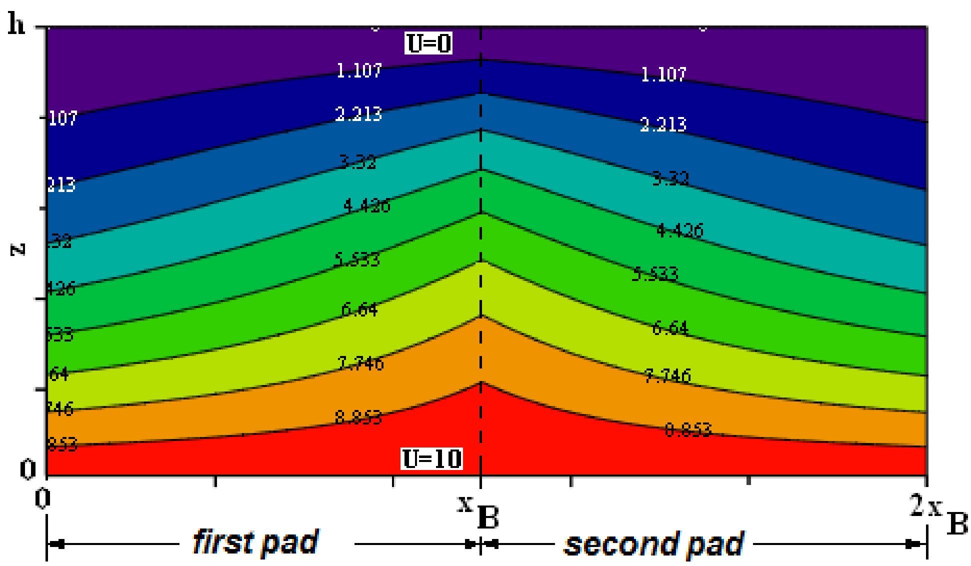

Figure 5. Speed distribution along the asperity in Figure 2

Figure 5 illustrates speed evolution from z=0, where fluid speed is 10 m/s, up to z=h, where speed annuls. It can be noticed that constant fluid speed occurs along approximately parallel contours, which confirms the considered hypothesis of laminar flow regime.

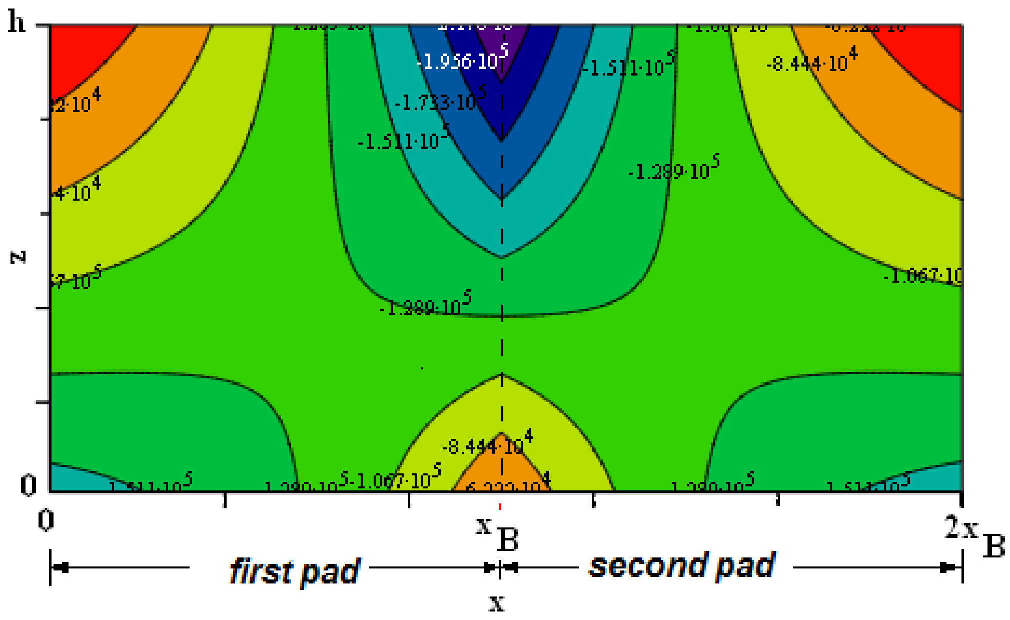

Figure 6. Shear stress distribution

Contours traced in the plot of shear stress distribution between plane and asperity represent constant stress levels (x_B - denotes the junction between the two pads).

2. LIMITING SHEAR STRESS ANALYSIS AND COMPARISON TO SHEAR STRENGTH

By analysis of shear stress distribution in a viscous Newtonian fluid that lubricates a plane pad bearing, it was determined that maxima are reached at boundaries, for $z=0$ and $z=h$, $z=h$ respectively:

$$\tau=\eta\frac{\partial u}{\partial z}; \qquad \tau=\frac{dp}{dx}\left(z-\frac{h}{2}\right)+\frac{\eta v}{h} \tag{0.28}$$

When particularized for the two pads forming the considered asperity, eq. (2.1) leads, under boundary conditions, to:

$$\tau_{1,z}=h=\frac{dp_1}{dx}\left(\frac{h_1}{2}\right)-\frac{\eta U}{h_1}; \qquad \tau_{2,z}=h=\frac{dp_2}{dx}\left(\frac{h_2}{2}\right)-\frac{\eta U}{h_2} \tag{0.29}$$

$$\tau_{1,z}=0=-\frac{dp_1}{dx}\left(\frac{h_1}{2}\right)-\frac{\eta U}{h_1}; \qquad \tau_{2,z}=0=-\frac{dp_2}{dx}\left(\frac{h_2}{2}\right)-\frac{\eta U}{h_2} \tag{0.30}$$

Thus, for the upper limit (asperity level):

$$\tau_z=h=\begin{cases}\tau_{1,z}=h, & 0<x<x_B\\ \tau_{2,z}=h, & x_B<x<2x_B\end{cases} \tag{0.31}$$

while for the lower limit (plane level):

$$\tau_z=0=\begin{cases}\tau_{1,z}=0, & 0<x<x_B\\ \tau_{2,z}=0, & x_B<x<2x_B\end{cases} \tag{0.32}$$

Shear distributions and shear strength were plotted on the same diagram, both positive and negative values, corresponding to the two pads, and comparisons were made.

$$\tau_{\lim 1} = \tau_{l0} + \beta p_1 \qquad \tau_{\lim 2} = \tau_{l0} + \beta p_2 \tag{0.33}$$

Limiting stress along the entire asperity pad can be determined by reunion of the two regions:

$$\tau_{\lim} = \begin{cases} \tau_{\lim 1}, & 0 < x < x_B \\ \tau_{\lim 2}, & x_B < x < 2x_B \end{cases} \tag{0.34}$$

In order to ensure good functioning of a lubricated bearing (EHL or HL), the stresses generated at the asperity limits must not exceed the shear strength (absolute value), [3]. By taking into consideration various speed and pad slope values, different situations were found from the ones modeled by Diaconescu, [4], [5], and Balan, in [6]. Particular situations, in which shear strength is reached, were then considered. To that end, the following variables were taken into consideration as input values:

- half-length of the base: $x_B = 0,025 \times 10^{-3} m$;
- minimum height of the lubricating film: $h_e = 0,0025 \times 10^{-3} m$;
- asperity height: $h_{rug} = 0,005 \times 10^{-3} m$;
- inlet to outlet ratio: $a = \dfrac{h_i}{h_e} = 3$;
- dynamic viscosity $\eta = 0,1 Pa \times s$;
- shear strength at atmospheric pressure: $\tau_{l0} = 1,2 \times 10^6 Pa$;
- shear strength to pressure ratio: $\beta = 0,15$;

Using the MathCad environment, both positive and negative values of limit shear stresses, and shear strength were plotted at plane speeds varying from $11 m/s$ up to $150 m/s$. Eight, most significant situations are illustrated in figures 7 - 14.

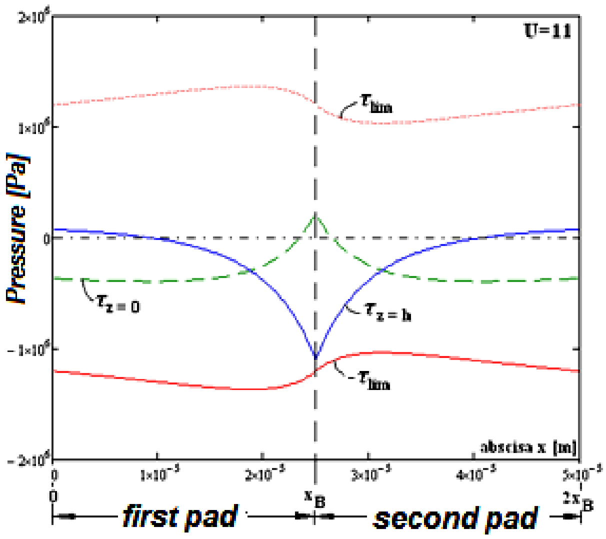

Fig. 7 Shear stress distribution for U = 11 m/s

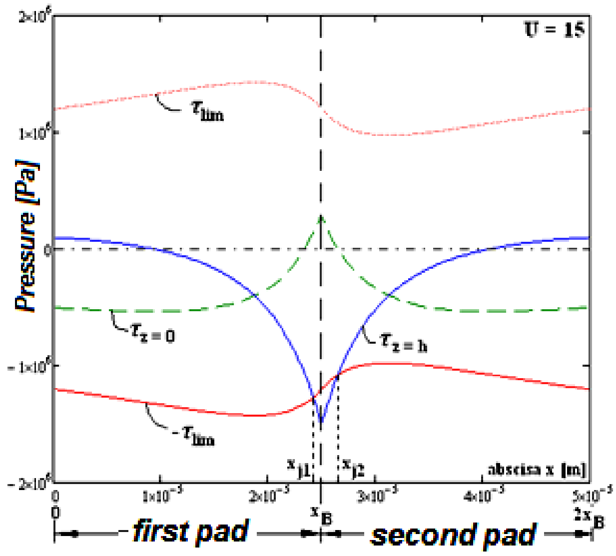

Fig. 8 Shear stress distribution for U = 15 m/s

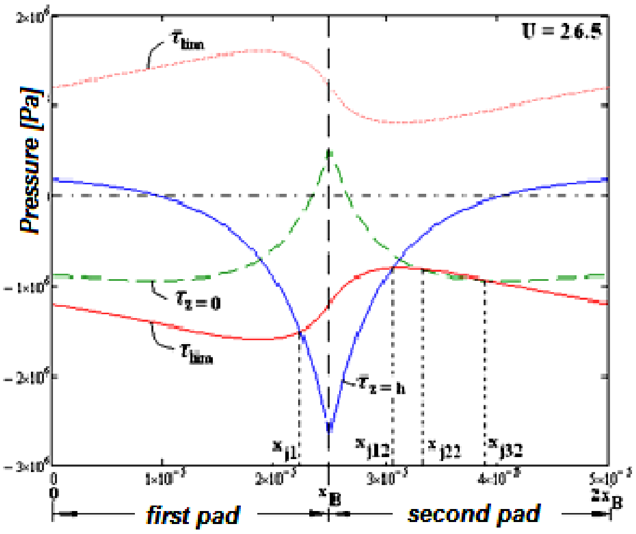

Fig. 9 Shear stress distribution for U = 26,5 m/s

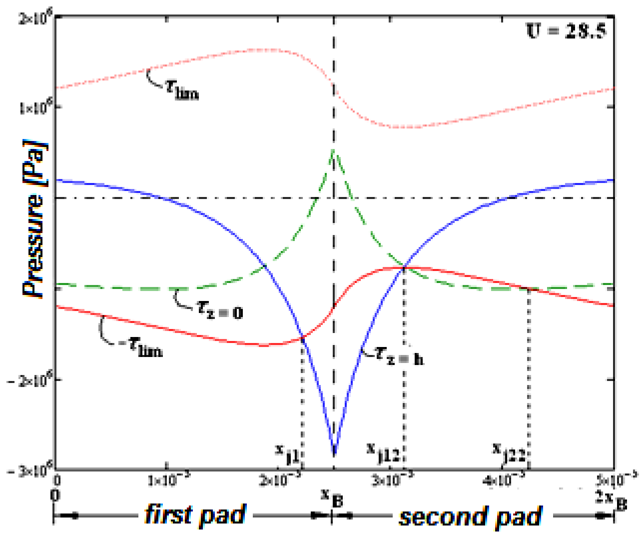

Fig. 10 Shear stress distribution for U = 28,5 m/s

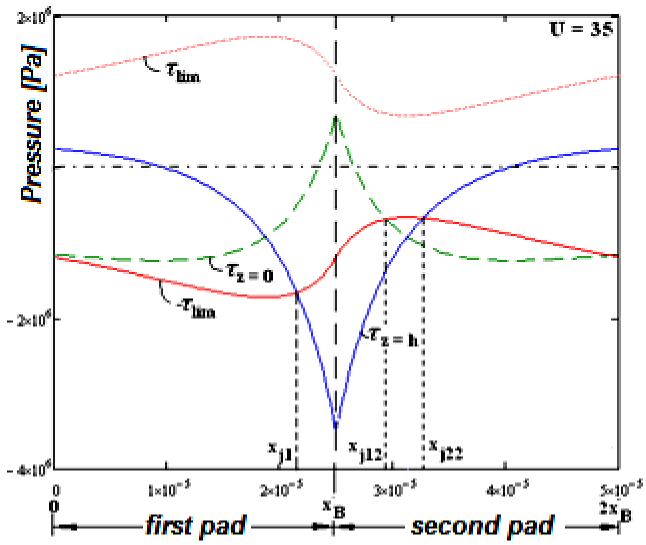

Fig.11 Shear stress distribution for U = 35 m/s

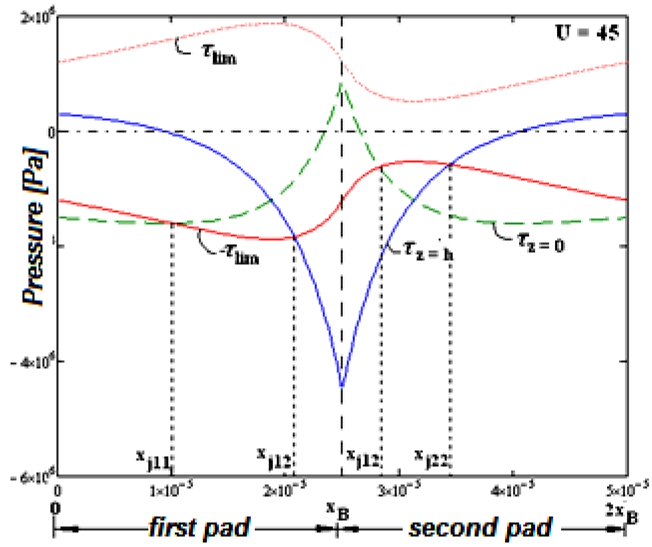

Fig.12 Shear stress distribution for U = 45 m/s

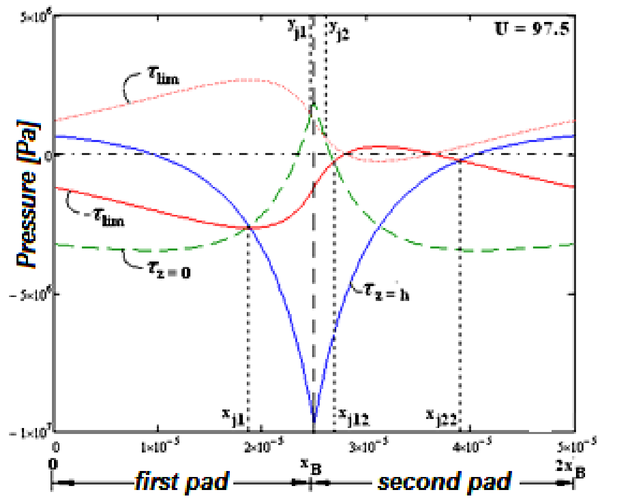

Fig. 13 Shear stress distribution for U = 97,5 m/s)

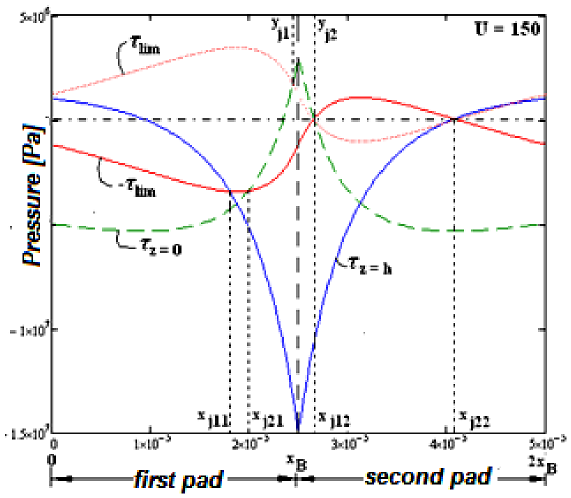

Fig. 14 Shear stress distribution for U = 150 m/s

3. DISCUSSION AND CONCLUSIONS

In the lubrication of a single asperity (simple triangular asperity, modeled as two symmetrical pads), from the point of view of geometric, cinematic and rheological parameters, eight significant situations can occur:

Case 1 (Figure 7): No plastic shear occurs. In this case, the fluid illustrates viscous Newtonian behavior;

Case 2 (Figure 8): Plastic shear occurs at the outlet of the firs pad, near the upper surface and at the inlet of the second pad near the upper surface;

Case 3 (Figure 9): Plastic shear occurs on the first pad in the vicinity of the upper surface and at the inlet of the second pad near the upper surface, as well as on the plane surface, corresponding to the second pad, between x_{j22} and x_{j32} abscissas;

Case 4 (Figure 10): For the first pad, plastic shear occurs at the outlet on the upper surface. For the second pad, three distinct regions appear: from the inlet to x_{j12}, plastic shear occurs on the upper surface; from x_{j12} to x_{j22}, plastic shear occurs on the lower surface; from to the outlet ($x = 2x_B$) he fluid illustrates viscous Newtonian behavior.

Case 5 (Figure 11): Plastic shear appears on the upper limit of the first pad and over the entire second pad, with an overlapping zone between x_{j12} and x_{j22};

Case 6 (Fig. 12): For the first pad, plastic shear occurs on the inlet lower limit and outlet upper limit, while for the second pad, a similar but much wider overlapping region appears as in ***Case 5.***

Case 7 (Figure 13): For the first pad, plastic shear regions unite in a single point, similar to the situation presented by Diaconescu in [4], [5]. For the second pad, plastic shear regions overlap.

Case 8 (Figure 14): Plastic shear occurs for both pads with overlapped regions, but for the second pad, the overlapping area is much wider.

After evaluating shear stresses that occur for each one of the presented cases, conclusions can be drawn regarding the influence of a single, asperity (simple, triangular) upon lubricant film plastic shear. From a pressure distribution point of view, appearance of a limiting shear stress leads to a decrease in “micro bearing capacity” (specific to a single asperity). If the problem is extended over the entire surface, the tips of singular asperities pass very close to each other, leading to very intense shearing in the lubricating film, which can lead to attaining the shear strength of the lubricating fluid film. If this situation occurs, local bearing capacity decreases drastically and asperities make contact, thus strongly increasing friction. This phenomenon can lead to seizing.

References:

[1] N. Popinceanu ş.a, Probleme fundamentale ale contactului cu rostogolire, Editura tehnica, Bucureşti, 1985

[2] I. Muscă, Implicaţii ale Reologiei în lubrificaţia EHD, Teză de Doctorat, Suceava 1996;

[3] P. Huang and S.Z. Wen, A New Model of Visco-Plastic Fluid Lubrication for Sliding Problems, Acta Tribologica, Vol. 2 pp 23-30 Suceava 1994, ISSN 1220-8434;

[4] E.N Diaconescu, Frecarea plastică izotermă a lubrifiantului în patina plană, 1996, Proceedings of 7th International Conference on Tribology, ROTRIB`96, vol. TCMM 18, 70-79.

[5] E.N Diaconescu, Upon Plastic Shear Zone in an Hydrodynamic Isothermal Flat Pad, 1996, Proceedings of VAREHD 8, ISBN 973-98210-8-1, pp. 239-248.

[6] M.Balan, Implicaţiile tensiunii limită de forfecare în lubrificaţie, Teza de Doctorat, Suceava ,2003.